UNIVERSITI PUTRA MALAYSIA

STRUCTURAL AND ELECTRICAL PROPERTIES OF CHEMICALLY-DOPED BARIUM ZINC NIOBATE PEROVSKITES

KRISHNAKUMAARY A/P KANNAN

FS 2021 61

STRUCTURAL AND ELECTRICAL PROPERTIES OF CHEMICALLY-DOPED BARIUM ZINC NIOBATE PEROVSKITES

By

KRISHNAKUMAARY A/P KANNAN

Thesis Submitted to the School of Graduate Studies, Universiti Putra Malaysia, in Fulfilment of the Requirements for the Degree of Master of Science

November 2020

Abstract of thesis presented to the Senate of Universiti Putra Malaysia in fulfilment of the requirement for the degree of Master of Science

STRUCTURAL AND ELECTRICAL PROPERTIES OF CHEMICALLY-DOPED BARIUM ZINC NIOBATE PEROVSKITES

By

KRISHNAKUMAARY A/P KANNAN

November 2020

Chairman : Tan Kar Ban, PhD
Faculty : Science

$Ba(Zn_{1/3}Nb_{2/3})O_3$ (BZN) perovskite has been recognised as an excellent dielectric material with moderately high dielectric constant ($\varepsilon' = 25$) and low dielectric loss, tan δ in the order of $\sim 10^{-1}$ at ~30 °C. BZN perovskite has a space group of *Pm3m* and unit formula of ($Z = 1$). Ba^{2+} and O^{2-} ions form a face-centred cubic unit cell whereas Zn^{2+} and Nb^{5+} ions occupy at the octahedral sites. In other words, $Ba(B^{2+}_{1/3}B^{5+}_{2/3})O_3$ has a combination of divalent and pentavalent cations with a ratio of 1:2 over the octahedral sites. In this work, an alkaline earth metal, Sr^{2+} and several transition metals, Ni^{2+}, Cd^{2+} and Ta^{5+} were successfully introduced into the BZN perovskite through solid-state reaction. Several solid solutions were prepared successfully with the proposed chemical formulas, $Ba_{(1-x)}Sr_xZn_{1/3}Nb_{2/3}O_3$ (BSZN), $BaZn_{(1/3-x)}B_xNb_{2/3}O_3$ (B = Ni and Cd) (BZNN and BZCN) and $BaZn_{1/3}Nb_{(2/3-x)}Ta_xO_3$ (BZNT), respectively. The solid solution limits of Sr-doped, Ni-doped, Cd-doped and Ta-doped BZN perovskites were determined to be $0 \leq x \leq 0.4$, $0 \leq x \leq 0.333$, $0 \leq x \leq 0.333$ and $0 \leq x \leq 0.67$, respectively. Interestingly, a complete substitutional solid solution range was found in the Cd-, Ni- and Ta-series. In this perspective, this could be due both isomorphous Nb^{5+} and Ta^{5+} have similar crystallochemical characteristics, e.g. similar charge and identical ionic radii (0.64 Å); therefore, these cations are interchangeable. Despite the relatively smaller ionic radii of Ni^{2+} (0.69 Å) and larger ionic radii of Cd^{2+} (0.95Å) than of Zn^{2+}(0.74 Å), these two dopants could fully replace Zn^{2+} at the 6-coordinated site. This may due to the overall large unit cell formed by a Ba^{2+} is large enough to accommodate these substitutions. These doped BZN solid solutions crystallised in a cubic symmetry with their lattice parameters, $a = b = c$ found to be in the range 4.0917(3)-4.1693(13) Å (Cd-series), 4.0917(3)-4.0786(6) Å (Ni-series), 4.0917(3)-4.0543(9) Å (Sr-series) and 4.0917(3)-4.1028(1) Å (Ta-series), respectively.

The linear correlation between lattice parameter and composition also showed that the Vegard's Law was obeyed. Both TGA and DTA analyses confirmed that all these doped BZN perovskites are thermally stable as neither phase transition nor weight loss was discernible over the studied temperature range ~30-1000°C. Meanwhile, the functional groups of the samples were identified by using FTIR in the wavenumber

range 250-1500 cm^{-1}. Besides that, the randomly distributed polyhedral grains of surface morphologies of these samples exhibiting a broad distribution of mean grain sizes with increasing dopant concentrations. Moreover, all these doped perovskites exhibited relatively larger crystallite sizes, as calculated by Williamson-Hall method, than those values determined by Scherrer method. The negligible small internal strain values showed the absence of structural deformation within all the doped perovskites. The Arrhenius conductivity plots of all these doped perovskites showed linear and reversible characteristics in a heating-cooling cycle. The activation energies of BZCN, BZNN, BSZN and BZNT perovskites are found in the range 2.51-3.19 eV, 2.44-3.19 eV, 2.13-3.19 eV and 1.71-3.19 eV, respectively. All the BZN perovskites appeared to be highly insulating with moderate low ε' and low tan δ at ~30 °C. The recorded ε' values of Cd-, Ni-, Sr- and Ta-series are in the range 24-29, 13-25, 15-25 and 19-27 respectively, at ~30 ºC and 1 MHz. The recorded tan δ values of BZCN-, BZNN-, BSZN- and BZNT-series were determined to be in the range 0.24-0.38, 0.22-0.36, 0.25-0.31 and 0.29-0.61, respectively, at ~30 ºC and 1 MHz.

In conclusion, $BaZn_{1/3}Nb_{2/3}O_3$ and doped materials were successfully synthesised by solid-state reaction method at the optimised conditions. All these doped materials exhibited interesting insulating properties at low temperature regions that may be due to high resistivity of grain boundary. The structural and electrical properties of chemically-doped barium zinc niobate perovskite had been demonstrated to be highly dependent on the composition and crystal structure.

Abstrak tesis yang dikemukakan kepada Senat Universiti Putra Malaysia sebagai memenuhi keperluan untuk Ijazah Master Sains

SIFAT STRUKTUR DAN ELEKTRIK TERDOP DALAM BARIUM ZINK NIOBATE PEROVSKIT SECARA KIMIA

Oleh

KRISHNAKUMAARY A/P KANNAN

November 2020

Pengerusi : Tan Kar Ban, PhD
Fakulti : Sains

$Ba(Zn_{1/3}Nb_{2/3})O_3$ (BZN) perovskit adalah dikenali sebagai bahan dielektrik yang sangat baik dengan pemalar dielektrik yang cukup tinggi ($\varepsilon' = 25$) dan kehilangan dielektrik rendah, tan δ dalam lingkungan $\sim 10^{-1}$ pada ~30 °C. BZN perovskit mempunyai kumpulan ruang *Pm3m* dan formula unit ($Z = 1$). Ion Ba^{2+} dan O^{2-} membentuk sel unit kubik berpusat muka sedangkan ion Zn^{2+} dan Nb^{5+} menempati di tapak oktahedral. Maka, $Ba(B^{2+}_{1/3}B^{5+}_{2/3})O_3$ mempunyai gabungan kation divalensi dan pentavalensi dengan nisbah 1: 2 di tapak oktahedral. Dalam kajian ini, logam alkali bumi, Sr^{2+} dan beberapa logam peralihan, Ni^{2+}, Cd^{2+} dan Ta^{5+} telah berjaya diganti ke dalam BZN perovskit melalui tindak balas keadaan pepejal. Beberapa larutan pepejal berjaya disediakan dengan menggunakan formula kimia yang dicadangkan seperti berikut, $Ba_{(1-x)}Sr_xZn_{1/3}Nb_{2/3}O_3$ (BSZN), $BaZn_{(1/3-x)}B_xNb_{2/3}O_3$ (B = Ni dan Cd) (BZNN dan BZCN) dan $BaZn_{1/3}Nb_{(2/3-x)}Ta_xO_3$ (BZNT). Julat larutan pepejal dalam Sr-, Ni-, Cd- dan Ta-dop BZN perovskit adalah $0 \leq x \leq 0.4$, $0 \leq x \leq 0.333$, $0 \leq x \leq 0.333$ dan $0 \leq x \leq 0.67$. Larutan pepejal yang lengkap telah terbentuk dalam siri Cd, Ni dan Ta. Dalam perspektif ini, kedua-dua isomorfus Nb^{5+} and Ta^{5+} mempunyai ciri kristalokimia yang serupanya, contohnya, mereka mempunyai cas ion dan saiz jejari ion yang sama (0.64 Å), oleh itu, kation ini boleh saling ditukarganti. Walaupun saiz jejari ion Ni^{2+} (0.69 Å) adalah lebih kecil dan saiz jejari ion Cd^{2+} (0.95Å) adalah lebih besar daripada Zn^{2+}(0.74 Å), dopan ini masih dapat menggantikan Zn^{2+} sepenuhnya di tapak yang berkoordinasi 6. Ini mungkin disebabkan keseluruhan sel unit yang dibentuk oleh Ba^{2+} cukup besar untuk menampung penggantian ini. Dopan BZN larutan pepejal ini menghablur dengan simetri kubik dengan parameter kekisi, $a = b = c$ didapati berada dalam linkungan 4.0917(3)-4.1693(13) Å (siri Cd), 4.0917(3)-4.0786(6) Å (siri Ni), 4.0917(3)-4.0543(9) Å (siri Sr) dan 4.0917(3)-4.1028(1) Å (siri Ta).

Sifat korelasi yang linear di antara parameter kekisi dengan komposisi menunjukkan bahawa Hukum Vegard telah dipatuhi. Kedua-dua analisis TGA dan DTA mengesahkan bahawa semua perovskit BZN adalah stabil secara terma memandangkan tiada sebarang peralihan fasa mahupun pengurangan berat yang diperhatikan dalam julat suhu ~30-1000 °C. Sementara itu, kumpulan berfungsi sampel dikenal pasti

dengan menggunakan FT-IR dalam julat bilangan gelombang 250-1500 cm^{-1}. Selain itu, morfologi permukaan untuk semua sampel-sampel dalam siri Cd, Ni, Sr dan Ta telah menunjukkan butiran yang tak sekata dan taburan purata saiz butiran yang luas dan semakin meningkat dengan kepekatan bahan pendop. Kesemua perovskit yang didopkan menunjukkan bahawa lebih besar saiz hablur yang ditentukan dengan kaedah Williamson-Hall, daripada nilai-nilai yang ditentukan oleh kaedah Scherrer. Nilai ketegangan dalaman adalah sangat kecil dan boleh diabaikan kerana ini menunjukkan tiada sebarang perubahan bentuk struktur yang ketara. Lakaran kekonduksian Arrhenius bagi perovskit yang didopkan telah menunjukkan ciri-ciri linear dan berbalik dalam kitaran pemanasan dan penyejukan. Tenaga pengaktifan untuk perovskit BZCN, BZNN, BSZN dan BZNT adalah dalam julat 2.51-3.19 eV, 2.44-3.19 eV, 2.13-3.19 eV and 1.71-3.19 eV. Semua perovskit BZN yang didopkan secara kimia ini mempunyai kerintangan yang tinggi dengan ε' yang sederhana rendah dan tan δ yang rendah pada suhu ~30 °C. Nilai-nilai ε' yang direkodkan oleh siri Cd, Ni, Sr dan Ta adalah dalam linkungan 24-29, 13-25, 15-25 dan 19-27 pada suhu ~30 ºC dan 1 MHz. Manakala, nilai tan δ yang direkodkan oleh siri BZCN, BZNN, BSZN dan BZNT ditentukan dalam linkungan 0.24-0.38, 0.22-0.36, 0.25-0.31, dan 0.29-0.61 pada suhu ~30 ºC dan 1 MHz.

Sebagai kesimpulannya, $BaZn_{1/3}Nb_{2/3}O_3$ dan bahan pendop berjaya disintesis melalui kaedah tindak balas keadaan pepejal pada keadaan yang optimum. Semua bahan terdop ini mempamerkan sifat kerintangan yang menarik pada lingkaran suhu rendah yang disebabkan oleh tinggi ketahanan sempadan butiran daripada butiran-butiran. Didapati juga, sifat struktur dan elektrik terdop dalam perovskite barium zink niobate adalah sangat bergantung terhadap komposisi bahan dan struktur hablur.

ACKNOWLEDGEMENTS

First and foremost, I would like to express my utmost gratitude to my project supervisor, Assoc. Prof. Dr. Tan Kar Ban for the continuous supports and being patience throughout the entire course of this project. I would like to extend my sincere appreciation to my co-supervisors, Dr. Khaw Chwin Chieh and Professor Dr. Zulkarnain Zainal for their guidance and ingenious suggestions.

I would like to thank the staff of the Department of Chemistry, UPM especially Madam Zainida Mohd Duad (XRD), Madam Nurhidayu Jamaludin (ICP-OES), Madam Nor Azlina Shari (TGA/DTA) and Madam Rusnani Amirudin (FTIR) for their technical assistance and guidance in data collection. I also would like express my sincere thanks to all the staff from the Electron Microscopy Unit, Institute of Bioscience (IBS) for their kind help.

My sincere thanks extend to my lab seniors, Ms. Nurul Aidayu bt Mat Dasin, Ms. Kartika binti Firman, Ms. Shafiqah Shaari, Ms. Rohayu Md Noor for all their guidance, helps and knowledge sharing in the beginning of my master journey. A special thanks to my cheerful friends in the lab 128, Ms. Farah Aishah Binti Jusoh, Mr. Athanenius Enteling and Ms. Vivian Loh Zing Ting who are always there for me whenever I have problems with the research and they help me a lot throughout my master journey.

Last but not least, my deepest gratitude goes to my beloved family members, especially my parents and my sisters for their encouragement, unflagging love and continuous support throughout my studies.

This thesis was submitted to the Senate of Universiti Putra Malaysia and has been accepted as fulfilment of the requirement for the degree of Master of Science. The members of the Supervisory Committee were as follows:

Tan Kar Ban, PhD
Associate Professor
Faculty of Science
Universiti Putra Malaysia
(Chairman)

Zulkarnain bin Zainal, PhD
Professor
Faculty of Science
Universiti Putra Malaysia
(Member)

Khaw Chwin Chieh, PhD
Associate Professor
Lee Kong Chian Faculty of Engineering and Science
Universiti Tunku Abdul Rahman
(Member)

_____
ZALILAH MOHD SHARIFF, PhD
Professor and Dean
School of Graduate Studies
Universiti Putra Malaysia

Date:

Declaration by Members of Supervisory Committee

This is to confirm that:

- the research conducted and the writing of this thesis was under our supervision;
- supervision responsibilities as stated in the Universiti Putra Malaysia (Graduate Studies) Rules 2003 (Revision 2012-2013) are adhered to.

Signature : _____
Name of Chairman of
Supervisory Committee : Assoc. Prof. Dr. Tan Kar Ban

Signature : _____
Name of Member of
Supervisory Committee : Prof. Dr. Zulkarnain Zainal

Signature : _____
Name of Member of
Supervisory Committee : Dr. Khaw Chwin Chieh

TABLE OF CONTENTS

LIST OF TABLES

LIST OF FIGURES

LIST OF ABBREVIATIONS

σ	conductivity
n	number of charge carriers
μ	the charge of the carrier
Z	carrier mobility
ρ	Resistivity
χ_m	magnetic susceptibility
H	applied magnetic field
T_C	Curie temperature
UHF	ultra high frequency
SHF	super high frequency
EHF	extremely high frequency
IoT	Internet of Things
3D	three dimensions
GPS	global positioning system
TV	television
ICs	integrated circuits
LTCC	low temperature co-fired ceramics
PCB	printed circuit board
ε'	real part of permittivity
$\tan \delta$	dielectric loss
Qf	quality factor
ε_o	free space permittivity
ε	permittivity of substances
ε''	imaginary part of permittivity

d	distance
μ	dipole moment
q	electron charge
P	Polarization
N	number of dipoles
τ_f	temperature coefficient of resonant frequency
ppm	parts per million
Z	unit formula
AFD	anti-ferrodistortive
SOJT	second-order Jahn–Teller
XRD	x-ray diffraction
SEM	scanning electron microscopy
HRTEM	high-resolution transmission electron microscopy
(c/a)	lattice constant ratio
Q_u	unloaded quality
FT-IR	fourier transform infrared spectroscopy
TGA	thermogravimetric analysis
DTA	differential thermal analysis
ICP-OES	inductively-coupled plasma–optical emission spectroscopy
AC	alternating current
a, b, c, α, β, γ	lattice parameters
λ	wavelength
ICDD	International Centre for Diffraction Data
TA	thermal analysis
ν	wavenumber

k	force constant
c	velocity of light
μ	reduced masses of atoms
ATR	Attenuated total reflectance
θ	Bragg angle
R	resistance
C	capacitance
Z^*	complex impedance
Y^*	complex admittance
M^*	complex modulus
ε^*	dielectric permittivity
ω	angular frequency
Z'	real part of impedance
Z''	imaginary part of impedance
Y'	real part of admittance
Y''	imaginary part of admittance
C_o	vacuum capacitance
M'	real part of electric modulus
M''	imaginary part of electric modulus
A	area
l	length
R_b	bulk resistance
R_{gb}	grain boundary resistance
C_b	bulk capacitance
C_{gb}	grain boundary capacitance
τ	relaxation time

f	frequency
GF	geometric factor
W-H	Williamson-Hall
ε	strain
FWHM	Full width of half-maximum
E_a	activation energy
IS	impedance spectroscopy
k_B	Boltzmann's constant
α	polarizability
r	ionic radii
t	tolerance factor

CHAPTER 1

INTRODUCTION

1.1 Electroceramics

The research in electroceramics has been driven by the growing demand in technological and device applications ranging from transportation, industrial production, medicine, power engineering, consumer electronics to communication (Setter and Waser, 2000). Electroceramics are also known as electronic ceramics that are used in a wide variety of electrical, optical and magnetic applications (Banerjee and Tyagi, 2012).

Over the past decades, the growth of various subclasses of electroceramics emerges parallel with the development of new technologies. For instance, high efficient energy storage and conversion devices, transducers, actuators, high dielectric constant capacitors and environmental monitoring device using semiconducting oxides are the key examples in various applications. The types of electroceramics include ceramic conductor, ceramic insulator, ceramic magnet, etc. The electroceramics are related to ceramics whose applications and properties are discussed in the subsequent sections 1.1.2 and 1.2, respectively.

1.1.1 What is Ceramic

The word ceramic is originated from the Greek keramos, which signifies “pottery” or “pottery’s clay”. Its origin is a Sanskrit term that means “to burn”. Early Greek used the term keramos to describe products produced by heating clay-containing materials. The term covers all the products produced from fired clay including bricks, fireclay refractories, sanitary-ware and tableware. These days, the word 'ceramic' has a more expansive significance and involves products such as glasses, advanced ceramics and certain cement systems (Carter and Norton, 2013).

Ceramics are an inorganic non-metallic solid made up of either metal or non-metal compounds that are formed and hardened by firing at high temperatures. Generally, ceramics are connected with “mixed” bonding, which is a combination of covalent, ionic and sometimes metallic. They consist of arrays of interconnected atoms where discrete molecules are absent. Oxides, nitrides and carbides are the most common ceramics. However, diamond and graphite are also classified as ceramics. Usually, they are hard, brittle and corrosion-resistant (Carter and Norton, 2013).

1.1.2 Common Applications of Electroceramics

Conductive ceramics are advanced materials that serve as electrical conductors due to the modifications in their structure. Most ceramics are able to withstand electrical current flow, which is why ceramic materials such as porcelains are traditionally

converted into electrical insulators. However, some ceramics are excellent electrical conductors and some are even superconductors. Most of these conductors are sophisticated ceramics whose properties are altered from powders to products through accurate processing control over their fabrication. The relative mobility of electrons within material is called as electric conductivity whereas, materials with higher mobility of electrons are known as conductors. Ceramic conductors are known to be one of the conductors which can maintain their mechanical integrity at high temperatures (> 1500 ºC). Ceramics exhibit the widest range of electrical properties of any of the classes of the material. The electrical conductivities of ceramics may vary over a wide range of values (over 24 magnitude orders) as shown in Figure 1.1.

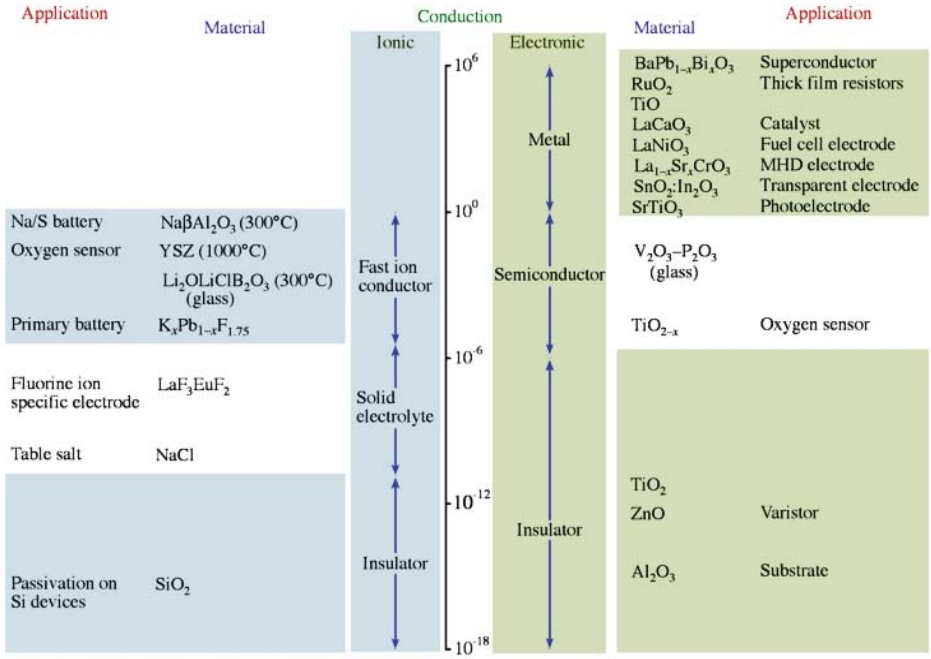

Figure 1.1: Typical range of ionic (left-hand side) and electronic (right-hand side) conductivities in ($\Omega^{-1}cm^{-1}$) exhibited by ceramics and their related applications (Carter and Norton, 2013)**.**

In general, there are two types of electric conductivity in ceramics which include both electronic and ionic conductions. Electronic conduction is passing through a material of free electrons. In ceramics, movement of free electrons is not allowed by the ionic bonds that hold the atoms together. However, the impurities of different valences, i.e. having different numbers of bonding electrons may be included in the material in some cases and these impurities may act as donors or electron acceptors. Electronically conductive ceramics are used as electrodes, resistors and heating elements. Meanwhile, ionic conduction consists of transiting ions (atoms of positive or negative charge) from one site to another through point defects, which are known as crystal lattice vacancies. Very little ion hopping takes place at normal ambient temperatures, as the atoms are in relatively low energy states. However, vacancies become mobile at elevated temperatures and some ceramics show what is known as fast ionic conduction. These

ceramics are particularly useful as fuel cells, gas sensors and batteries. The general factors affecting electrical conductivity (σ) are the number of charge carriers, n, the charge of the carrier, μ and carrier mobility, Z, which are formulated in the equation below:

$$\sigma = nZe\mu \tag{1.1}$$

On the contrary, insulators can be described as high resistivity products. Insulators are mainly used to keep conductive components in position and to prevent them from getting into contact with each other. There is a wide energy gap between the bottom of the conduction band and the top of the valence band in an electrical insulator. Many ceramics and indeed electroceramics are considered as good electrical insulators in nature and several ceramics have resistivity, ($\rho > 10^{14}$ Ωcm), which can resist the flow of current and able to separate charge as a result. Examples of common ceramic insulators are porcelain (clay), aluminum oxide, cristobalite porcelain, mullite, forsterite, beryllium oxide, boron nitride and aluminum nitride (Carter and Norton, 2013).

Over the past six decades, ceramic magnets have become strongly established as electrical and electronic engineering materials; most of them contain iron as an important component and are known collectively as 'ferrites'. Ampère, Savart, Biot and Oersted were among the first to demonstrate that conductors carrying currents produced magnetic fields and exerted 'Lorentz' forces on each other (Moulson and Herbert, 2003). Magnetic ceramic materials possess great properties such as low loss characteristics, strong magnetic coupling and high electrical resistivity, which are mostly required to fabricate new devices for applications. Magnetic ceramics are the main material for various applications such as tunnel junction, spin valve, data storage and high frequency application. Magnetic materials can be categorised as diamagnetic, paramagnetic or ferromagnetic based on their magnetic susceptibilities. The magnetic susceptibility (χ_m) is a measure of the degree of magnetisation of a material in an applied magnetic field (Moulson and Herbert, 2003). Diamagnetic materials have a very small negative susceptibility (about 10^{-6}-10^{-5}) such as inert gases, hydrogen, metals, non-metals and organic compounds. In these cases, the electron movements are such that they produce a zero net magnetic moment (Figure 1.2a). When a magnetic field is applied to a diamagnetic material, the electron movements are changed and a small net magnetisation is produced in a way that is opposite to the field applied (Figure 1.2b).

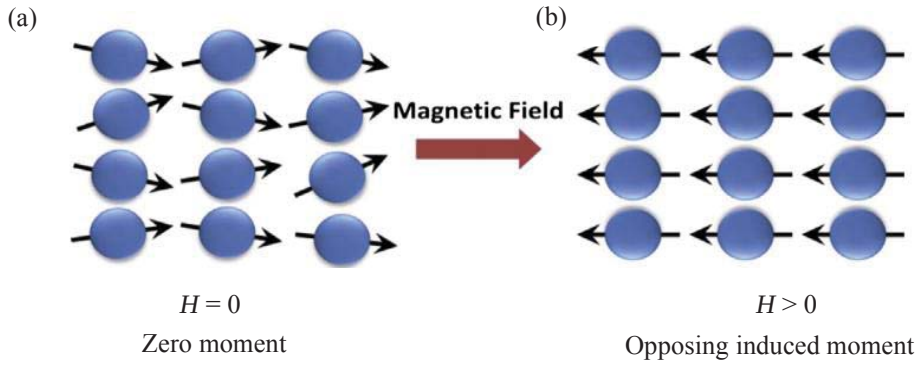

Figure 1.2: The atomic dipole configuration for a diamagnetic material (a) without and (b) with an applied magnetic field (*H*) (Kotnala and Shah, 2015)**.**

On the other hand, paramagnetic is the substance in which the atoms have a permanent magnetic moment resulting from spinning and orbiting electrons, i.e. unpaired electron. In the absence of a magnetising field, the electron's magnetic moments are randomly distributed and the net magnetic moment per unit volume is zero (Figure 1.3a). An applied field tends to orient the moments, so the resulting field is produced in the same way as the applied field (Figure 1.3b). Therefore, the susceptibilities are positive but small, commonly in the range 10^{-3}-10^{-6} (Barsoum, 1997).

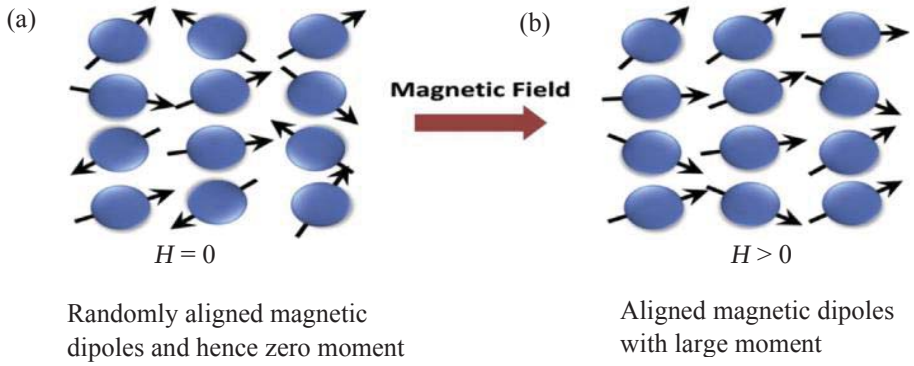

Figure 1.3: The atomic dipole configuration for a paramagnetic material (a) without and (b) with an applied magnetic field (*H*) (Kotnala and Shah, 2015)**.**

Ferromagnetic materials are very related to paramagnetic materials when it comes to permanent magnetic moments. Ferromagnetic materials contain ordered domains or regions of single magnetic moment orientation, which give rise to large finite magnetisation in the absence of a magnetic field. Ferromagnetic materials exhibit a strong magnetism in the same direction of the field when a magnetic field is applied. Ferromagnetism is only possible when atoms are arranged in the lattice and the atomic magnetic moments can interact to align parallel to each other (Figure 1.4). Ferromagnetic materials are spontaneously magnetised below a critical temperature,

which is known as Curie temperature, above which the materials act like a paramagnetic material and the magnetic susceptibility is large (below T_C) (Barsoum, 1997).

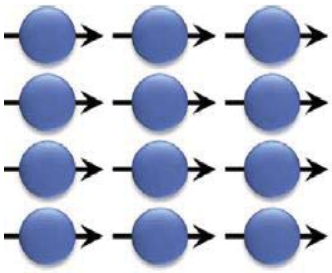

Figure 1.4: Schematic representation of spins in a ferromagnetic material (Kotnala and Shah, 2015)**.**

1.1.3 Dielectric Materials

A dielectric ceramic is an electrically insulating material or a very poor conductor of electricity in which a positive and negative charged entities could be separated by an applied electric field. When a dielectric is placed in the electrical field, the electrical charges do not flow through the material as they do in the electrical conductor, but only slightly shift away from their average balance positions, causing the dielectric polarisation. Due to this, positive charges are shifted in the direction of the field and negative charges are shifted in the opposite direction to the field. This produces an internal electrical field that decreases the overall field within the dielectric field itself. If a dielectric is composed of weakly bonded molecules, those molecules not only become polarised but also reorient so that their symmetry axes align with the field. An ideal dielectric material does not show electrical conductivity when an electric field is applied. In reality, all dielectrics do exhibit some conductivities, which normally increase with increasing temperature and applied field (Bain and Chand, 2007). The term dielectric is used to indicate the energy storing capacity of a material. An example of a dielectric is placing a ceramic material between the metallic plates of a capacitor. If the voltage across the dielectric material becomes too high, or if the electrostatic field becomes too strong, the material would unexpectedly begin to conduct current. This process is called dielectric breakdown.

An essential property of a dielectric is its capability to support an electrostatic field while dissipating minimum energy in the form of heat. The lower the dielectric loss of a material, the more efficient this dielectric material. Another thing which comes into consideration is the dielectric constant, which explains the extent to which a substance concentrates the electrostatic lines of flux. Some of the materials with a low dielectric constant are perfect vacuum, dry air, most pure and dry gases like helium and nitrogen. Materials with moderate dielectric constants include ceramic, glass, distilled water, etc. Moreover, metal oxides usually have high dielectric constants. The study of dielectric properties are related to the storage and dissipation of electric and magnetic energy in

materials. Dielectrics are important for explaining various phenomena in electronics, optics and solid-state physics (Billah, 2018).

1.1.4 Dielectric for Microwave Applications

Microwaves are a form of electromagnetic radiation with wavelength ranging from about 1 meter to 1 millimetre; with frequencies between 300 MHz (1 m) and 300 GHz (1 mm) (Bingham and Cohrssen, 2004). In the electromagnetic spectrum, microwave region ranges between 0.3 to 300 GHz (Figure 1.5). This broad range can be divided into three parts such as ultra high frequency (UHF), super high frequency (SHF) and extremely high frequency (EHF), which are found in the range (0.3 to 3 GHz), (3 to 30 GHz) and (30 to 300 GHz), respectively. In this region, wavelength approximates the physical size of common electronic components and has been found to act differently at microwave frequency than at a lower frequency. Microwave dielectric ceramics are utilised in both mobile telecommunication handsets and base station filtering technologies. Most importantly, the microwave dielectric materials play a significant role in a global society for a wide range of applications from terrestrial and satellite communications, including Internet of Things (IoT), software radio, antennas, GPS and direct broadcast satellite TV, to environmental monitoring via satellite, etc. (Sebastian *et al.*, 2015; Scotta, e*t al*., 2003).

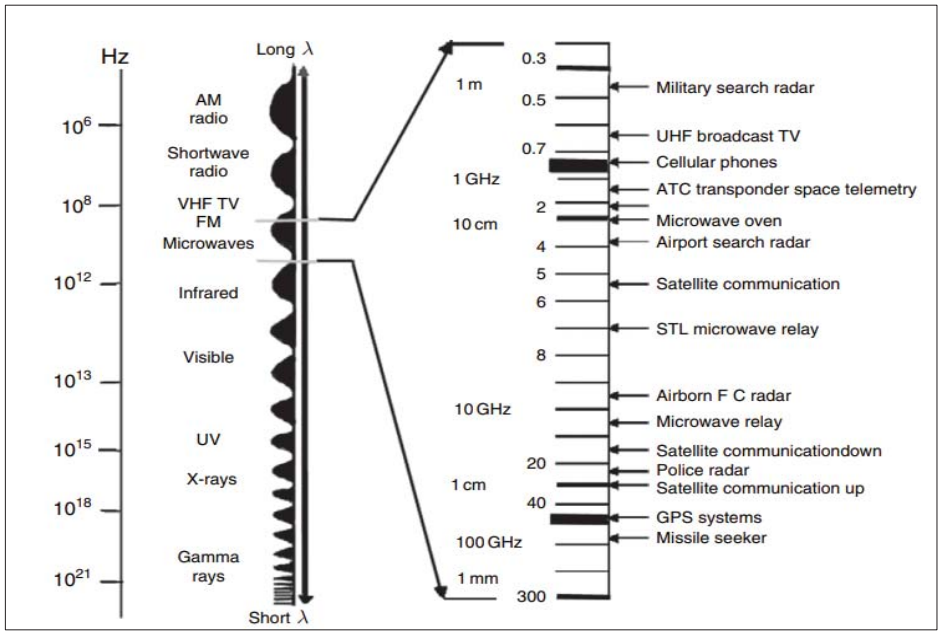

Figure 1.5: Microwave spectra and applications (Sebastian, 2008)**.**

1.1.4.1 Substrates

Substrates are a base material on which processing is conducted to produce new films or layers of material such as deposited coatings. Ceramic substrate technologies in the electronic business are always considered in the sense of "ceramic printed boards" or

more precisely as film integrated circuits. Ceramic substrates are widely used in the field of microelectronic packaging, sensors and actuators and passive components (Bechtold, 2009). In the process of electronic packaging, the substrates mainly play the role of electrical interconnection (insulation) and mechanical support protection. With the development of electronic packaging technology towards miniaturised devices, which uses up fewer resources, with more energy efficient, high density, cost less, multi-function and high reliability, the power density of the electronic system increases and the heat dissipation issue become more serious. Several factors may influence the heat dissipation of devices, among which the selection of substrate materials appears to be a key factor. Moreover, the savings in weight and space through miniaturisation are a stimulus for creating devices with even higher performance (Sömiya, 1984).

Recently, there are four main types of substrate materials generally used in electronic packagings such as ceramic substrate, metal substrate, polymer substrate and composite substrate. The ceramic substrate material is widely used in electronic packaging substrate due to its advantages such as high strength, good insulation, small thermal expansion coefficient, good chemical stability, low sodium ion content, low cost, good thermal conductivity and heat resistance. The ceramic substrate materials used include alumina, beryllium oxide, aluminium nitride, silicon carbide and mullite. In terms of structure and manufacturing process, ceramic substrates can be divided into low-temperature co-firing ceramic substrates, high-temperature co-fired multi-layer ceramic substrates, thick film ceramic substrates, etc. Substrates and packages for integrated circuits (ICs) are the largest applications for ceramic insulators (Sömiya, 1984). On the other hand, the metal substrates are notable for their very high thermal conductivity compared to ceramics and polymers substrates. It also used as a heat sink for power devices. These are some examples of substrate materials of metals, e.g. aluminum, copper and gold. The polymer substrates, e.g. polyimide is electrically insulating similar to the ceramic substrate but the polymer substrates seem to have lower dielectric constant than ceramic substrates. The composite materials are a combination of materials that can be modified either to improve mechanical and thermal behavior, or as an electrical conductor (Kasap and Capper, 2007; Ramdani, 2019).

1.1.4.2 Low Temperature Co-fired Ceramics (LTCC)

Currently, LTCC has become more crucial in the development of various modules and substrates. This technology combined various thin layers of low-permittivity ceramic composites and conductors and the resulting multi-layered LTCC modules are commonly applied in the form of 3D wiring circuit board today. The LTCC permits a versatile mix of passive microwave components such as microstrips, antennas, filters, striplines, resonators, inductors, capacitors, phase shifters and dividers, thus making possible a whole matrix of design that are not practical on regular alumina or any soft substrates. Moreover, these integrated components are interconnected with 3D stripline circuitry. Among the various components that could be realised in LTCC packages are resonators and internal capacitors, which are essential in terms of the latest technology (Sebastian, 2008).

The great advantage of LTCC technology is the low sintering temperature (< 950 ºC) as this provides the advantageous utilisation for today's packaging concepts in

microelectronic and microwave modules. Therefore, this features embedded microwave components and transmission lines that can be fabricated using highly conductive and inexpensive metals, e.g. gold, silver, or copper with low conductor loss and low electrical resistance at high-frequencies. LTCC also features the ability of embedding passive elements, e.g. resistors, capacitors and inductors into the ceramic package, thus minimising the size of the completed module (Sebastian, 2008).

1.1.4.3 Printed Circuit Boards (PCB)

A printed circuit board (PCB) is a sheet for the attachment of chips, whether mounted on substrates, chip carriers, or otherwise and for the drawing of interconnections. It is a polymer-matrix composite that is electrically insulating and has four conductor lines (inter-connections) on one or both sides. Multilayer boards have lines on each inside layer so that inter-connections on different layers may be connected by short conductor columns called electrical vias. PCB boards or cards for the mounting of pin-inserting-types packages need to have lead insertion holes punched through the circuit board. Printed circuit boards for the mounting of surface-mounting-type packages need no holes. The main ingredients in a PCB composite are the polymer matrix, e.g. epoxy and reinforcing fibers, e.g. glass and kelvar. The conventional method of fabricating a PCB includes the lamination of fiber prepregs. In addition to the interconnection, metal layers and columns may be incorporated in a board to restrict the thermal expansion and heat dissipation such as metal columns which are known as thermal vias (Chung *et al.*, 1995).

1.2 Dielectric Properties

The study of dielectric properties involved with the storage and dissipation of electric and magnetic energy in materials. In practice, most dielectric materials are solid such as porcelain (ceramic), glass, mica, plastics and oxides of various metals. Dielectrics are also used as insulation for wires, cables and electrical equipment, polarisable media for capacitors and a variety of artifacts, e.g. rectifiers, semiconductor devices, piezoelectric transducers, memory elements and dielectric amplifiers (Bain and Chand, 2017).

Dielectric materials have the unique property of being capable to store electrostatic charges (Anderson *et al.*, 1990). Invariably, they are substances in which electrons are localised in the process of bonding the atoms together. Therefore, covalent or ion bonds, or a combination of both, or van der Waals bonding between closed-shell atoms, all these give rise to solids (or gasses) displaying dielectric properties. The dielectric properties of a ceramic material determine its functionality. These properties include dielectric constant (ε'), dielectric loss (tan δ) and quality factor (Qf).

1.2.1 Dielectric Constant

The dielectric constant or relative permittivity of the material shows its energy storing capacity when a potential is applied across. It is related to the macroscopic properties such as polarisation or capacitance. For circuit miniaturisation, generally one employs a

high dielectric constant material. The permittivity of a material also determines the relative speed that an electrical signal can pass through in the material. A low permittivity will result in a high signal propagation speed (Sebastian, 2008).

Relative permittivity or dielectric constant, ε' is the ratio of the permittivity of a substance to the permittivity of space or vacuum. While dielectric constant can be expressed as below:

$$\varepsilon' = \varepsilon/\varepsilon_{\circ} \quad (1.2)$$

The absolute permittivity, ε_o is the measure of the resistance of a substance when it encounters a formation of the electric field. Dielectric constant exhibits the relative permittivity value of vacuum or free space, ε_o where ε_o is 8.854 x 10^{-12} Fm^{-1} and the ε shows the permittivity of some substances (Sebastian, 2008).

Generally, there are several categories of dielectric material depending on the magnitude of dielectric constant, which are low permittivity (ε' up to 15), medium permittivity (ε' between 15 and 500) and high permittivity (ε' between 500 and 20,000). Low- and medium-permittivity dielectrics are known as Class I dielectrics, whereas high-permittivity materials are called Class II dielectrics. A third class (Class III) contains a conductive phase that can be very useful, as it decreases the thickness of the dielectric in capacitors. Besides, the ceramic insulators include silicates and aluminas, which are used for low-permittivity ceramic dielectrics. Meanwhile, titanium dioxide (titania) can be used to modify low and medium permittivity classes especially for the microwave resonator and low-loss stable capacitor. The high permittivity dielectric material such as barium metatitanate ($BaTiO_3$), could be used as a substitute for mica in a capacitor (Nanni *et al.*, 1999).

1.2.2 Dielectric Loss

The dielectric loss (tan δ) of a material indicates the quantitative dissipation of the electrical energy due to various physical processes, e.g. dielectric relaxation, electrical conduction, dielectric resonance and losses from non-linear processes. The origin of dielectric losses may be linked to delay between the electric field and the electric displacement vector. The total dielectric loss is the combination of intrinsic and extrinsic losses. Intrinsic dielectric losses are the losses in the perfect crystals that depend on the crystal structure and can be described by the interaction of the phonon system with the ac electric field. The intrinsic dielectric losses depend on crystal symmetry, ac field frequency and temperature. These intrinsic losses fix the lower limit of losses in defect-free single crystals or ideal pure materials. On the other hand, extrinsic losses are related to imperfections in the crystal lattice like impurities, grain boundaries, microstructural defects, porosity, microcracks, order-disorder, random crystallite orientation, dislocations. vacancies, dopant atoms, etc. (Sebastian, 2008). The dielectric loss can be portrayed using the formula as follow:

$$\tan \delta = \varepsilon'' / \varepsilon' \quad (1.3)$$

where ε'' is the imaginary part of the permittivity; ε' is the relative permittivity which termed as loss factor. The tan δ is usually taken as an indication of the quality of a

specific type of capacitor. Generally, a high loss dielectric is not suitable in almost all applications. It reduces the quality and results in the generation of heat that increases the temperature of a capacitor.

1.2.3 Quality Factor

The term "quality factor" is more generally related to microwave resonators. The quality factor is a measure of the power loss of a microwave system. For a microwave resonator, losses can be of four types such as dielectric, conduction, radiation and external. The measurement conditions can be adjusted such that the losses due to conduction and radiation can be neglected. Sometimes the quality factor of an insulation portion is determined, that is, the value reciprocal of the loss tangent:

$$Q = 1 / \tan \delta \tag{1.4}$$

The values of tan δ for the best electrical insulating materials used in high-frequency and high-voltage engineering practices are of the order of thousands and even tenths of thousands of fractions (Sebastian, 2008).

1.3 Polarisation

Although no charge is transferred when a dielectric is placed in an electrical field, there is a redistribution of the charge that occurs via the formation and movement of electrical dipoles. There is an associated dipole moment, μ, having both magnitude and direction:

$$\mu = qd \tag{1.5}$$

where d is the separation of the positive and negative ends of the dipole and q is an electron charge. The dipole direction is, by convention, taken to the point from the negative end to the positive end.

When a dielectric material is placed in an electric field, the induced dipoles and any permanent dipoles become aligned. The material is now said to be polarised and the polarisation (or dipole moment per unit volume) is given by:

$$P = Nqd \tag{1.6}$$

where N is the number of dipoles. Generally, there are four types of polarisation mechanisms in a dielectric material and the details for each mechanism are explained in the next section (Carter and Norton, 2013). The polarisation gives rise to useful behavior, like as electrical energy storage (capacitors) and the conversion between electrical energy and mechanical energy (piezoelectric effect) (Chung, 2010).

1.3.1 Types of Polarisation

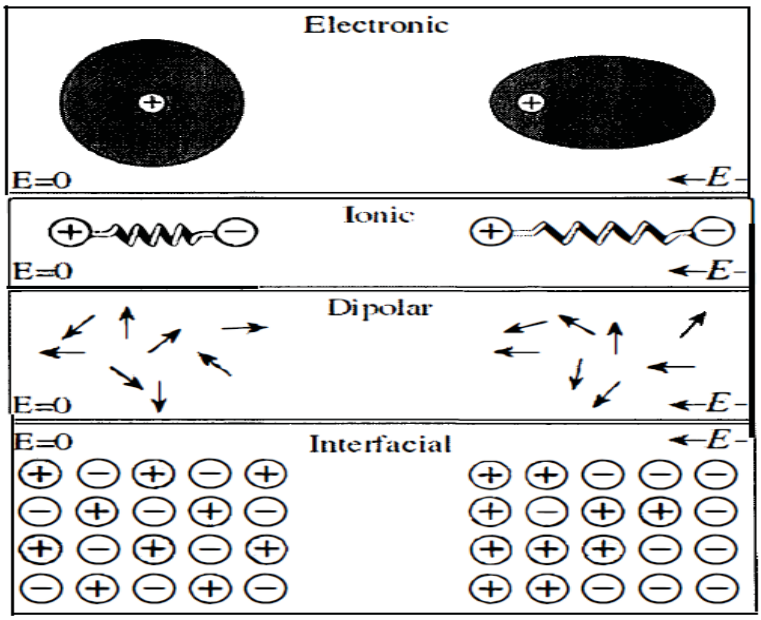

Figure 1.6: Illustration of the different polarisation mechanisms in a solid (Carter and Norton, 2013)**.**

a) Electronic Polarisation

When an electric field is applied to an atom, there is a displacement of the electrons relative to the nucleus. The electrons concentrate on the side of the nucleus near the positive end of the field. The atom acts as a temporarily induced dipole. This effect occurs in all materials (because all materials contain atoms), but the magnitude is small because the distance (d) is very small. Electronic polarisation is the only possible mechanism in pure materials that are covalently bonded and do not contain permanent dipoles (e.g. diamond, silicon). The electronic polarisation occurs at high frequencies of about 10^{-16} Hz (Carter and Norton, 2013).

b) Ionic Polarisation

Ionic polarisation, which happens when an ionically bonded material is placed in an electric field, is common in many ceramics, e.g. MgO, Al_2O_3, NaCl. The bonds between the ions are elastically deformed. Consequently, the charge is minutely redistributed. Depending on the direction of the field, the cations and anions move either closer together or further apart. These temporarily induced dipoles cause polarisation and may also change the overall dimensions of the material. The dipole moment is usually small because, once again, the displacements involved are very small. The mechanism contributes to the relative permittivity at infrared frequency range about ~10^{12} -10^{-13} Hz (Carter and Norton, 2013).

c) Dipolar or Orientation Polarisation

This type of polarisation involves the orientation of the permanent dipoles, if present in the lattice without an electric field. In zero electric field, the dipoles will be randomly oriented, thus carrying no net polarisation. When an electric field is applied, the dipoles will tend to align in the direction of the applied field and the materials will acquire a net moment. This is known as an orientation polarisation. The orientation time of this polarisation is much longer which they remain within 10^{-8}-10^{-10} Hz (Carter and Norton, 2013; Nowotny and Rekas, 1992).

d) Interface or Space Charge Polarisation

A charge may develop at interfaces, e.g. grain or phase boundaries and free surfaces, normally as a result of the presence of impurities. The charge moves on the surface when the material is placed in an electric field. This type of polarisation is not well understood, although it has a considerable practical interest because most real materials and in particular, many ceramics are not pure (Carter and Norton, 2013).

1.4 Problem Statement

Nowadays, the increasing demand for renewable energy is due to the growing concerns on the depletion of non-renewable energy resources, e.g. fossil fuels and environmental pollution problems. Although the non-renewable energy is easily accessible, the formation may take millions of years through the natural process. On the other hand, sufficient sunlight and wind could be utilised for solar and wind energy; however, the set-up would be very costly and complicated. These reasons have triggered much research impetus in searching for high performance materials and fabricating devices, which are capable of storing, absorbing and supplying the electricity. In general, the electric energy storage devices could be divided into two classes: (i) the long-term energy storage time, e.g. battery, which has high energy density but low power density; (ii) the short term one, e.g. capacitor, which has high power density but low energy density. With the rapid development of power electronics, dielectric materials with low dielectric loss, high dielectric constant, high energy storage density and good thermal stability are highly demanded for a wide variety of applications. In this context, perovskite materials are one of the potential candidates due to their great flexibility in terms of composition and structure. These materials also show a wide range of electrical properties, e.g. semiconducting, high insulating and/or superconducting. $Ba(Zn_{1/3}Nb_{2/3})O_3$ (BZN) perovskites have been recognised as an excellent type I dielectric material with moderate high dielectric constant ($\varepsilon' = 41$) and low temperature coefficient of resonant frequency ($\tau_f = 30$ ppm/°C), which mostly used in electronics as microwave resonators and/or micro/radio-wave filters. By far, barium magnesium tantalate (BMT), barium magnesium niobate (BMN) and barium zinc tantalate (BZT) are well known to be used as dielectric materials, which are applicable for microwave technological devices. To date, only limited information is available in literature regarding the electrical properties of the BZN perovskites in microwave region. Therefore, a detailed study of BZN perovskites is highly beneficial to further understand and explore their potentials in a wider frequency range. This research emphasises on synthesis and characterisation of novel perovskite phases in the BZN ternary system. On the other hand, suitable chemical dopants (Cd^{2+}, Ni^{2+}, Sr^{2+} and Ta^{5+})

were introduced into the system to enhance the electrical properties of BZN materials. The selection of these dopants is due to the reasons including: (i) same oxidation state with Ba^{2+}, Zn^{2+} and Nb^{5+} and (ii) size of ionic radius that suits the requirement of relatively large *A* site and smaller *B* site, which is expected to improve the dielectric properties. The compositions with excellent electrical properties will be made into a suitable form for prototype testing prior to commercial application.

1.5 Objectives

The key objectives of this work are outlined as below:

a) To synthesise single phase parent barium zinc niobate ($BaZn_{1/3}Nb_{2/3}O_3$) perovskite by solid-state reaction and characterise the pure phase material by using XRD, FTIR, SEM, TGA, DTA, ICP and AC impedance spectroscopy.

b) To synthesise and characterise chemically doped $Ba_{(1-x)}Sr_xZn_{1/3}Nb_{2/3}O_3$ (BSZN), $BaZn_{(1/3-x)}B_xNb_{2/3}O_3$ (*B* = Ni and Cd) (BZNN and BZCN) and $BaZn_{1/3}Nb_{(2/3-x)}Ta_xO_3$ (BZNT) perovskites.

c) To study their phase compatibility, solid solubility and thermal stability.

d) To investigate the effects of different dopants on the structural and electrical properties of BZN perovskites and doped materials using AC impedance spectroscopy.

REFERENCES

Abram, E.J., Sinclair D.C. and West A.R. 2001. Electrode-contact spreading resistance phenomena in doped-lanthanum gallate ceramics. *Journal of Electroceramics* 7(3): 179-188.

Akbas, M.A. and Davies, P.K. 1998. Cation ordering transformations in the $Ba(Zn_{1/3}Nb_{2/3})O_3$-$La(Zn_{2/3}Nb_{1/3})O_3$ system. *Journal of the American Ceramic Society* 81(4): 1061-1064.

Alkathy, M.S., Gayam, R. and James Raju, K.C. 2017 Effect of nickel and lithium co-substituted barium titanate ceramics on structural and dielectric properties. *Journal of Materials Science: Materials in Electronics* 28: 1684-1694.

Anderson, J.C., Leaver, K. D., Rawlings, R. D. and Alexander, J. M. 1990. Dielectrics, In *Materials Science*, ed J. C. Anderson, K. D. Leaver, R. D. Rawlings and J. M. Alexander, pp 518-549. Springer, Boston, MA.

Azough, F., Leach, C. and Freer, R. 2004. Effect of cation order on microwave dielectric properties of $Ba(Zn_{1/3}Nb_{2/3})O_3$ ceramics. *Key Engineering Materials* 264-268: 1153-1156.

Bain, A.K. and Chand, P. 2017. Dielectric properties of material. In *Ferroelectrics: Principles and Applications*, ed. A.K. Bain and P. Chand, pp 1-18. Wiley-VCH Verlag GmbH &Co. KGaA.

Banerjee, S. and Tyagi, A.K. 2012. Electroceramics for fuel cells, batteries and sensors. In *Functional Materials: Preparation, Processing and Applications*, ed. S. Banerjee and A.K. Tyagi, pp 639-674. Elsevier.

Barsoum, M. 1997. Magnetic and nonlinear dielectric properties. In *Fundamentals of ceramics*, ed. M. Barsoum, pp 507-551.The McGraw-Hill Companies, Singapore.

Barve, A.K., Gadegone, S.M., Lanjewar, M.R. and Lanjewar, R.B. 2014. Synthesis and characterization of CdO nanomaterial and their photocatalytic activity. *International Journal on Recent and Innovation Trends in Computing and Communication* 2(9): 2806-2810.

Barwick, M., Azough, F. and Freer, R. 2006. Structure and dielectric properties of perovskite ceramics in the system $Ba(Ni_{1/3}Nb_{2/3})O_3$-$Ba(Zn_{1/3}Nb_{2/3})O_3$. *Journal of the European Ceramic Society* 26:1767-1773.

Batoo, K.M., Kumar, S., Lee, C.G. and Alimuddin. 2009. Influence of Al doping on electrical properties of Ni–Cd nano ferrites. *Current Apllied Physics* 9: 826-832

Baud, G., Picaud, B. and Besse, J.P. 1975. New series of rhenium perovskite compounds of $Ba_4M_3ReO_{12}$ type. *Journal of American Ceramic Society* 58: 259.

Bechtold, F. 2009. A comprehensive overview on today's ceramic substrate technologies. *2009 European Microelectronics and Packaging Conference*, 1-12. https://ieeexplore.ieee.org/document/5272912

Bhalla, A.S., Guo, R. and Roy, R. 2000. The perovskite structure – a review of its role in ceramic science and technology. *Material Research Innovation* 4: 3-26.

Billah S.M. (2018). Dielectric Polymers. In *Functional Polymers*. ed. S.M. Billah, pp 1-49. Springer, Cham.

Bingham, E. and Cohrssen, B. 2004. Radio-frequency and microwave radiation. In *Patty's Toxicology*, ed. R.T. Hitchcock, pp 133-165. Wiley-Backwell.

Bose, S.C. and Nag, A. 2016. Effect of dual-doping on the thermoelectric transport properties of $CaMn_{1/x}Nb_{x/2}Ta_{x/2}O_3$. *RSC Advances* 6: 52318-52325.

Carter, C.B. and Norton, M.G. 2013. Background you need to know. In *Ceramic Materials: Science and Engineering*, ed. C.B. Carter and M.G. Norton, pp 37-52. New York: Springer Science + Business Media, Inc.

Carter, C.B. and Norton, M.G. 2013. Conducting charge or not. In *Ceramic Materials: Science and Engineering*, ed. C.B. Carter and M.G. Norton, pp 545-572. New York: Springer Science + Business Media, Inc.

Carter, C.B. and Norton, M.G. 2013. Introduction. In *Ceramic Materials: Science and Engineering*, ed. C.B. Carter and M.G. Norton, pp 3-13. New York: Springer Science + Business Media, Inc.

Carter, C.B. and Norton, M.G. 2013. Locally redistributing charge. In *Ceramic Materials: Science and Engineering*, ed. C.B. Carter and M.G. Norton, pp 573-592. New York: Springer Science + Business Media, Inc.

Çetinörgü-Goldenberg, E., Klemberg-Sapieha, J-E. and Martinu, L. 2012. Effect of postdeposition annealing on the structure, composition, and the mechanical and optical characteristics of niobium and tantalum oxide films. *Applied Optics* 51(27): 6498-6507.

Chauhan, L., Shukla, A.K. and Sreenivas, K. 2015. Dielectric and magnetic properties of Nickel ferrite ceramics using crystalline powders derived from DL alanine fuel in sol–gel auto-combustion. *Ceramics International* 41(7); 8341-8351.

Chen, X.M. and Wu, Y.J. 1996. Dielectric characteristics of $Ba(Mg_{1/3}Ta_{2/3})O_3$ ceramics sintered at low temperatures. *Journal of Materials Science: Materials in Electronics* 7: 427-431.

Chung, D.D.L. 1995. Electronic packaging materials and their functions in thermal managements. In *Materials for Electronic Packaging*, ed. D.D.L. Chung, pp 131-167. Butterworth-Heinemann.

Chung, D.D.L. 2010. Dielectric Behavior. In *Functional materials: electrical, dielectric, electromagnetic, optical and magnetic applications: and*

companion solution manual, ed. D. D. L. Chung, pp 95-200, World Scientific Publishing Co. Pte, Ltd.

Collins, B.M., Jacobson, A.J. and Fender, B.E.F. 1974. Preparation of the ordered perovskite-like compounds $Ba_4M_3LiO_{12}$ (M = Ta, Nb): A powder neutron diffraction determination of the structure of $Ba_4Ta_3LiO_{12}$. *Journal of Solid State Chemistry*, 10(1): 29-35.

Das, R., Sarkar, T. and Mandal, K. 2012. Multiferroic properties of Ba^{2+} and Gd^{3+} co-doped bismuth ferrite: magnetic, ferroelectric and impedance spectroscopic analysis. *Journal of Physics D: Applied Physics* 45: 455002.

Das, T., Das, B.K., Parashar, K. and Parashar, S.K.S. (2016). Temperature and frequency dependence electrical properties of $Zn_{1-x}Ca_xO$ nanoceramic. *ACTA Physica Polonica A* 130(6): 1358-1362.

Dasari, M.P., Godavarti, U. and Mote, V. 2018. Structural, morphological, magnetic and electrical properties of Ni-doped ZnO nanoparticles synthesized by co-precipitation method. *Processing and Application of Ceramics* 12(2); 100-110.

Dasin, N.A.M., Tan, K.B., Khaw, C.C., Zainal, Z. and Chen, S. K. 2017. Subsolidus solution and electrical properties of Sr-substituted bismuth magnesium niobate pyrochlores. *Ceramics International* 43(13): 10183-10191.

Dasin, N.A.M., Tan, K.B., Zainal, Z., Khaw, C.C., and Chen, S.K. 2019. Doping mechanisms and impedance study of Ba-substituted bismuth magnesium niobate pyrochlores. *Journal of Electroceramics* 43: 41-50.

Davies P.K., Tong J. and Negas T. 1997. Effect of ordering-induced domain boundaries on low-loss $Ba(Zn_{1/3}Ta_{2/3})O_3$-$BaZrO_3$ perovskite microwave dielectrics. *Journal of the American Ceramic Society* 80(7): 1727-1740.

Davies, P.K. and Roth, R.S. 1991. Chemistry and properties of temperature compensated microwave dielectrics. In *Chemistry of Electronic Ceramic Materials*, ed. T. Negas, G. Yeager, S. Bell and R. Amren, pp. 21-34. Technomic Publishing Co. Inc., Lancaster, PA, USA.

Davies, P.K., Borisevich A. and Thirumal, M. 2003. Communicating with wireless perovskites: cation order and zinc volatilization. *Journal of the European Ceramic Society* 23: 2461-2466.

Davies, P.K., Wu, H., Borisevich, A.Y., Molodetsky, I.E. and Farber, L. 2008. Crystal chemistry of complex perovskites: new cation-ordered dielectric oxides. *Annual Review of Materials Research* 38: 369-401.

Desu, S.B. and O'Bryan, H.M. 1985. Microwave loss quality of $Ba(Zn_{1/3}Ta_{2/3})O_3$ ceramics. *Journal of American Ceramic Society* 68(10): 546-551.

Dias, A. and Moreira, R.L. 2003. Far-infrared spectroscopy in ordered and disordered $BaMg_{1/3}Nb_{2/3}O_3$ microwave ceramics. *Journal of Applied Physics* 94(5): 3414-3421.

Dong, H. and Shi, F. 2012. Effect of synthesis temperature on crystal structure and phonon modes of $Ba[Zn_{1/3}(Nb_{0.4}Ta_{0.6})_{2/3}]O_3$ ceramics. *CrystEngComm* 14(23): 8268-8273.

Dong, H.L. and Shi, F. 2011. Vibration spectra and structural characteristics of $Ba[(Zn_{1-x}Mg_x)_{1/3}Nb_{2/3}]O_3$ solid solutions. *Applied Spectroscopy Reviews* 46(3): 207-221.

Endo, K., Fujimoto, K. and Murakawa, K. 1987. Dielectric properties of ceramics in $Ba(Co_{1/3}Nb_{2/3})O_3$-$Ba(Zn_{1/3}Nb_{2/3})O_3$ solid solutions. *Journal of American Ceramic Society* 70: 215-218.

Fielicke, A., Meijer, G. and Von Helden,G. 2003. Infrared multiple phonon dissociation spectroscopy of transition metal oxide cluster cations. *European Physical Journal D: Atomic, Molecular, Optical and Plasma Physics* 24: 69-72.

Firman, K., Tan, K.B., Khaw, C.C., Zainal, Z., Tan, Y.P. and Chen, S.K. 2017. Doping mechanisms and electrical properties of bismuth tantalate fluorites. *Journal of Materials Science* 52(17): 10106-10118.

Furukawa, O., Yamashita, Y., Harata, M., Takahashi, T. and Inagaki, K. 1985. Dielectric properties of modified lead zinc niobate ceramic. *Japanese Journal of Applied Physics* 24(3): 96-99.

Galasso, F.S. and Pyle, J. 1963. Ordering in compounds of the $A(B'_{0.33}Ta_{0.67})O_3$ type. *Inorganic Chemistry* 23: 482-484.

Galasso, F.S. and Pyle, J. 1963. Preparation and study of ordering in $A(B'_{0.33}Nb_{0.67})O_3$ perovskite type compounds. *Journal of Physical Chemistry* 67: 1561-1562.

Galasso, F.S., Barrante, J.R. and Katz, L. 1961. Alkaline earth tantalum oxygen phases including the crystal structure of an ordered perovskite compound $Ba_3SrTa_2O_9$. *Journal of American Chemical Society* 83: 2830-2832.

Glazer, A.M. 2011. A brief history of tilts. *Phase Transitions* 84(5-6): 405-420.

Gouda, M.E., Badr, S.K., Hassan, M.A. and Sheha, E. 2011. Impact of ethylene carbonate on electrical properties of PVA/$(NH_4)_2SO_4$/H_2SO_4 proton-conductive membrane. *Ionics* 17: 255-261.

Grebennikov, D. and Mascher, P. 2011. Structural properties of near-stoichiometric composition of $Ba(B'_{1/3}\ B''_{2/3})O_3$ (B' = Mg, Co, or Zn and B'' = Nb or Ta) perovskites. *Journal of Materials Research and Technology* 26(9): 1116-1125.

Han, L., Christensen, D.V., Bhowmik, A., Simonsen, S. B., Hung, L.T., Abdellahi, E., Chen, Y.Z., Nong, V., Linderoth, S. and Pryds, N. 2016. Scandium-doped zinc cadmium oxide as a new stable n-type oxide thermoelectric material. *Journal of Material Chemistry A* 4(31): 12221-12231.

Hazen, R.M. 1988. Perovskites. *Scientific American* 258(6): 74-81.

Hernández, A., Maya, L., Mora, E.S. and Sanchez, E.M. 2007. Sol-gel synthesis, characterization and photocatalytic activity of mixed oxide ZnO-Fe_2O_3. *Journal of Sol-Gel Science and Technology* 42: 71-78.

Hikichi, Y., Chen, Z., Newnham, R.E. and Cross, L.E. 1982. Preparation, thermal change and dielectric properties of cubic perovskites $A(B_{1/4}Nb_{3/4})O_3$ (A = Ba or Sr, B = Na or Li). *Materials Research Bulletin* 17: 1371-1377.

Himanshu, A.K., Choudhary, B.K., Gupta, D.C. Bandyopadhayay, S.K. and Sinha, T.P. 2010. Impedance spectroscopy of perovskite barium substituted lead zinc niobate ceramics. *Physica B* 405(6): 1608-1614.

Himanshu, A.K., Choudhary, B.K., Singh, S.N., Gupta, D.C., Bandyopadhayay, S.K. and Sinha, T.P. 2010. Synthesis and dielectric relaxation studies of Ba substitution in $Pb(Zn_{1/3}Nb_{2/3})O_3$ ceramics by co-precipitation method. *Solid State Sciences* 12: 1231-1234.

Hong, K-S., Kim, I,T. and Kim, C.D. 1996. Order–disorder phase formation in the complex perovskite compounds $Ba(Ni_{1/3}Nb_{2/3})O_3$ and $Ba(Zn_{1/3}Nb_{2/3})O_3$. *Journal of the American Ceramic Society* 79: 3218-3224.

Hoque, M.M., Dutta, A., Kumar, S. and Sinha, T.P. 2014. Dielectric Relaxation and Conductivity of $Ba(Mg_{1/3}Ta_{2/3})O_3$ and $Ba(Zn_{1/3}Ta_{2/3})O_3$. *Journal of Material Science and Technology* 30(4): 311-320.

Huang, C. L., Hsu, C. S. and Liu, S. J. 2003. Dielectric properties of $0.95Ba(Zn_{1/3}Nb_{2/3})O_3$–$0.05BaZrO_3$ ceramics at microwave frequency. *Materials Letters* 57(22-23): 3602-3605.

Ianculescu, A., Brăileanu, A., Voicu, G. and Stoleriu, Ş. 2007. Phase formation mechanism and characteristics of strontium barium niobate ceramics. *Journal of the European Ceramic Society* 27: 517-521.

Ioachim, A., Toacsan, M.I., Banciu, M.G., Nedelcu, L., Dutu, C.A., Feder, M., Plapcianu, C., Lifei, F. and Nita, P. 2007. Effect of the sintering temperature on the $Ba(Zn_{1/3}Ta_{2/3})O_3$ dielectric properties. *Journal of the European Ceramic Society* 27(2-3): 1117-1122.

Irvine, J.T.S., Sinclair, D.C. and West, A.R. 1990. Electroceramics: characterisation by impedance spectroscopy. *Advance Materials* 2(3): 132-138.

Jaafar, H., Ahmad, Z.A. and Ain, F. 2011. Effects of calcination temperature on the phase formation and microstructure of barium zinc tantalate. *Advanced Materials Research* 173: 61-66.

Jacobson, A.J., Collins, B.M. and Fender, B.E.F. 1976. A powder neutron and X-ray diffraction determination of the structure of $Ba_3Ta_2ZnO_9$: an investigation of perovskite phases in the system Ba-Ta-Zn-O and the preparation of $Ba_2TaCdO_{5.5}$ and $Ba_2CeInO_{5.5}$. *Acta Crystallographica* 32:1083-1087.

Kang, S.G., Kim, H., Takahashi, K. and Tsukioka, M. 1994. Synthesis and properties of (1-x)PZN-xBZN solid-solution compounds by liquid-evaporation method. *Japanese Journal of Applied Physics* 33: 5407-5411.

Kasap, S. and Capper, P. (2007). Packaging materials. In *Springer Handbook of Electronic and Photonic Materials*. ed S. Kasap and P. Capper, pp 1267-1285, New York: Springer Science + Business Media, Inc.

Kaur, B., Singh, L., Reddy, V.A., Jeong D.Y., Dabra, N. and Hundal, J.S. 2016. AC impedance spectroscopy, conductivity and optical studies of Sr doped bismuth ferrite nanocomposites. *International Journal of Electrochemical Science* 11: 4120-4135.

Kawashima, S., Nishida, M., Ueda, I. and Ouchi, H. 1983. $Ba(Zn_{1/3}Ta_{2/3})O_3$ ceramics with low dielectric loss at microwave frequencies. *Journal of American Ceramic Society* 66: 421-423.

Khatri, P., Behara, B., Srinivas, V. and Choudhary, R.N.P. 2008. Complex impedance spectroscopic properties of $Ba_3V_2O_8$ ceramics. *Research Letters in Materials Science* :1-6.

Khirade, P.P., Shinde, A.B., Raut, A.V., Birajdar, S.D. and Jadhav, K.M. 2016. Investigations on the synthesis, structural and microstructural characterizations of $Ba_{1-x}Sr_xZrO_3$ nanoceramics. *Ferroelectrics* 504: 216-229.

Kibasomba, P.M., Dhlamini, S., Maaza, M., Liu, C-P., Rashad, M.M., Rayan, D.A. and Mwakikunga, B.W. 2018. Strain and grain size of TiO_2 nanoparticles from TEM, Raman spectroscopy and Xrd: the revisiting of the williamson-hall plot method. *Results in Physics* 9: 628-635.

Kim I-T., Hong, K.S. and Yoon S-J. 1995. Effects of non-stoichiometry and chemical inhomogeneity on the order-disorder phase formation in the complex perovskites compounds, $Ba(Ni_{1/3}Nb_{2/3})O_3$ and $Ba(Zn_{1/3}Nb_{2/3})O_3$. *Journal of Materials Science* 38: 514-521.

Kim, B.K., Hamaguchi, H., Kim, I.T. and Hong, K-S. 1995. Probing of 1:2 ordering in $Ba(Ni_{1/3}Nb_{2/3})O_3$ and $Ba(Zn_{1/3}Nb_{2/3})O_3$ ceramics by XRD and Raman spectroscopy. *Journal of the American Ceramic Society* 78: 3117-3120.

Kim, E.S. and Yoon, K.H. 1992. Microwave dielectric properties of complex perovskite $Ba(Mg_{1/3}Ta_{2/3})O_3$. *Ferroelectrics* 133: 187-192.

Kim, E.S. and Yoon, K.H. 1994. Effect of nickel on microwave dielectric properties of $Ba(Mg_{1/3}Ta_{2/3})O_3$. *Journal of Materials Science* 29(3): 830-834.

Kim, I.T., Kim, Y.H. and Chung, S.J. 1997. Ordering and microwave dielectric properties of $Ba(Ni_{1/3}Nb_{2/3})O_3$ ceramics. *Journal of Materials Research* 12: 518-525.

Kim, I.T., Kim, Y. H. and Chung, S. J., 1995. Order–disorder transition and microwave dielectric-properties of $Ba(Ni_{1/3}Nb_{2/3})O_3$ ceramics. *Japanese Journal of Applied Physics* 1(34): 4096-4103.

Kim, J., Suh, D., Kim, N. and Kim, H. 2004. Dielectric properties of 0.08Pb $[(Mg_{1/3}Ta_{2/3}),(B'_{1/3}B''_{2/3})]O_3-0.2PbTiO_3$ ceramics ($B'B''$ = ZnTa, MgNb and ZnNb). *Journal of the American Ceramic Society* 87(7): 1250-1253.

Kim, M-H., Naim. S., Lee, W-S., Yoo, M-J., Park, J-C. and Lee, H-J. 2004. Effect of microstructure on microwave dielectric properties of Al_2O_3-added $Ba(Zn_{1/3}Ta_{2/3})O_3$ ceramics. *Japanese Journal of Applied Physics* 43(4A): 1438-1441.

Kolodiazhnyi, T. 2012. $BaMg_{1/3}Nb_{2/3}O_3$-$Mg_4Nb_2O_9$ composite microwave ceramics with high *Q*-factor and low sintering temperature. *Journal of the European Ceramic Society* 32(16): 4305-4309.

Kolodiazhnyi, T., Petric, A., Belous, A., V'yunov, O. and Yanchevskij, O. 2002. Synthesis and dielectric properties of barium tantalates and niobates with complex perovskite structure. *Journal of Materials Research* 17(12): 3182-3189.

Koster, G., Huijben, M. and Rijnders, G. 2015. The effects of strain on crystal structure and properties during epitaxial growth of oxides. In *Epitaxial Growth of Complex Metal Oxides*. ed. G. Koster, M. Huijben and G. Rijnders, pp 175-207. Woodhead Publishing Series in Electronic and Optical Materials.

Kotnala, R. K., and Shah, J. 2015. Ferrite materials: nano to spintronics regime. *Handbook of Magnetic Materials* 23: 291-379.

Lee, C.T., Lin, Y.C., Huang, C.Y., Su, C.Y. and Hu, C.L. 2007. Cation ordering and dielectric characteristics in barium zinc niobate. *Journal of the American Ceramic Society* 90(2): 483-489.

Lee, Y.C., Liang, M.H., Hu, C.T. and Lin, I.N. 2001. Microwave dielectric properties of $Ba(Mg_{1/3}Ta_{2/3})O_3$ materials synthesized by inverse-microemulsion process. *Journal of the European Ceramic Society* 21(15): 2755-2758.

Leśniak, M., Szal, R., Starzyk, B., Gajek M., Kochanowicz, M., Żmojda, J., Miluski, P., Dorosz, J., Sitarz, M. and Dorosz, D. 2019. Influence of barium oxide on glass-forming ability and glass stability of the tellurite–phosphate oxide glasses. *Journal of Thermal Analysis and Calorimetry* 138: 4295-4302.

Lim, J-B., Kim, D-H., Nahm, S., Paik, J-H. and Lee, H-J. 2006. Effect of B_2O_3 and CuO additives on the sintering temperature and microwave dielectric properties of $Ba(Mg_{1/3}Nb_{2/3})O_3$ ceramics. *Materials Research Bulletin* 41(6): 1199-1205.

Liu, S., Taylor, R., Petrovic, N.S., Budd, L., Schifgaarde, M.V. and Newman, N. 2005. Experimental and theoretical investigation of the structural, chemical, electronic, and high frequency dielectric properties of barium cadmium tantalate–based ceramics. *Journal of Applied Physics* 97(1): 1-8.

Ma, P.P., Yi, L., Liu, X.Q., Li, Q.L. and Chen, X.M. 2013. Effects of Mg substitution on order/disorder transition, microstructure, and microwave dielectric characteristics of $Ba((Co_{0.6}Zn_{0.4})_{1/3}Nb_{2/3})O_3$ complex perovskite ceramics. *Journal of American Ceramic Society* 96(6): 1795-1800.

Macdonald, J.R. and Johnson, W.B. 2005. Fundamentals of impedance spectroscopy. In *Impedance Spectroscopy-Theory, Experiment, and Applications*, ed. J.R. Macdonald and W.B. Johnson, pp 1-26. New Jersey: Wiley-Interscience.

Mandal, B. and Thakur, A.K. 2018. AC impedance spectroscopy of NASICON type $Na_3Fe_2(PO_4)_3$ ceramic. *AIP Conference Proceedings*. 1953(1). 050018.

Mangai, K.A., Selvi, K.T., Priya, M., Rathnakumari, M., Sureshkumar, P. and Sagadevan, S. 2017. Investigations on dielectric and impedance properties of M-type hexaferrite. *Journal of Materials Science: Materials in Electronics* 28: 2910-2922.

Manivannan, S., Chandra, V.S.S., Sharma, P.K., Raju, K.C.J. and Das, D. 2014. Effect of flux addition on mechanical and microwave dielectric properties of barium zinc tantalate ceramics. *Transactions of the Indian Ceramic Society* 73(2): pp 87-89.

Manivannan, S., Joseph, A., Sharma, P.K., Raju, K.C.J. and Das, D. 2017. Effect of colloidal processing on densification and dielectric properties of $Ba(Zn_{1/3}Ta_{2/3})O_3$ ceramics. *Ceramic International* 43(15): 12658-12666.

Matsubara, M., Kikuta, K. and Hirano, S. 2005. Piezoelectric properties of $(K_{0.5}Na_{0.5})(Nb_{1-x}Ta_x)O_3$-$K_{5.4}CuTa_{10}O_{29}$ ceramics. *Journal of Applied Physics* 97: 114105.

Matsumoto, H., Tamura, H. and Wakino, K. 1991. $Ba(Mg,Ta)O_3$-$BaSnO_3$ high-*Q* dielectric resonator. *Japanese Journal of Applied Physics* 30(9B): 2347-2349.

Mergen, A., Sahin, E.I., Kent, S., Kartal, M. and Mohammed, J.E.F. 2019. Effect of Ni and Sb substitution on the dielectric properties $Ba(Zn_{1/3}Nb_{2/3})O_3$ ceramics. *Conference: sustainable materials science and technology* : 1-15. https://www.researchgate.net/publication/331928437

Moulson, A.J. and Herbert, J.M. 2003. Magnetic ceramics. In *Electroceramic: Materials, Properties, Applications*, ed. A.J. Moulson and J.M. Herbert, pp 469-546. New York: John Wiley & Sons, Ltd.

Muller, O. and Roy, R. 1974. The ABX_3 structures. In *The major ternary structural families*. ed. O. Muller and R. Roy, pp 46. New York: Springer-Verlag Berlin Heidelberg

Nanni, P., Viviani, M., and Buscaglia, V. 1999. Synthesis of dielectric ceramic materials. *Handbook of Low and High Dielectric Constant Materials and their Applications* 1:429-455.

Negas, T., Roth, R.S., Parker, H.S. and Brower, W.S. 1973. Crystal chemistry of lithium in octahedrally coordinated structures. I. Synthesis of $Ba_8(Me_6Li_2)O_{24}$ (Me = Nb or Ta) and $Ba_{10}(W_6Li_4)O_{30}$. *Journal of Solid State Chemistry* 8: 1-13.

Nomura, S. 1983. Ceramics for microwave dielectric resonator. *Ferroelectrics* 49: 61-70.

Nomura, S., Toyama, K. and Kaneta, K. 1982. $Ba(Mg_{1/3}Ta_{2/3})O_3$ ceramics with temperature- stable high dielectric constant and low microwave loss. *Japanese Journal of Applied Physics* 21(10): 624-626.

Nowotny, J. and Rekas, M. 1992. Dielectric ceramic materials based on alkaline earth metal titanates. *Key Engineering Materials* 66-67: 45-144.

Padmamalini, N. and Ambujam, K. 2016. Impedance and modulus spectroscopy of ZrO_2-TiO_2-V_2O_5 nanocomposite. *Karbala International Journal of Modern Science* 2; 271-275.

Paik, J-H., Kim, S-K., Lee, M-J., Choi, B-H., Lim, E-K. and Nahm, S. 2006. Ordering structure of barium magnesium niobate ceramic with A-site substitution. *Journal of the European Ceramic Society* 26: 2885-2888.

Pawlak, D.A., Ito, M., Dobrzycki, L., Wozniak, K., Oku, M., Shimamura, K. and Fukuda, T. 2005. Structure and spectroscopic properties of $(AA')(BB')O_3$ mixed-perovskite crystals. *Journal of Materials Research* 20: 3329-3337.

Phatungthane, T., Jaita, P. and Rujijanagul, G. 2019. Structural, dielectric and impedance study on ZnO doped $Sr(Fe_{0.5}Nb_{0.5})O_3$ ceramics. *Physica B: Condensed Matter* 556: 103-107.

QingQing, P., Ping, G., Jiong, D., Qiang, C. and Hui, L. 2012. Comparative crystal structure determination of griseofulvin: powder x-ray diffraction versus single-crystal x-ray diffraction. *Chinese Science Bulletin* 57(30): 3867-3871.

Qasrawi, A.F., Sahin, E.İ., Emek, M., Kartal, M. and Kargin, S. 2019. Structural and dielectric performance of the $Ba(Zn_{1/3}Nb_{2/3-x}Sb_x)O_3$ perovskite ceramics. *Materials Research Express* 6(9): 095095.

Rahdar, A., Aliahmad, M. and Azizi, Y. 2015. NiO Nanoparticles: Synthesis and Characterization. *Journal of Nanostructures* 5: 145-151.

Ramdani, N. (2019). Mechanical properties of polymer/ceramic composites. In *Polymer and Ceramic Composite Materials: Emergent Properties and Applications*. ed N. Ramdani, pp 93-128, CRC Press Taylor & Francis Group.

Rayssi, C., El.Kossi, S., Dhahri, J. and Khirouni, K. 2018. Frequency and temperature-dependence of dielectric permittivity and electric modulus studies of the solid solution $Ca_{0.85}Er_{0.1}Ti_{1-x}Co_{4x/3}O_3$ ($0 \leq x \leq 0.1$). *RSC Advances* 8: 17139-17150.

Rodrigues, J.E.F.S., Castro, P.J., Pizani, P.S., Correr, W.R. and Hernandes, A.C. 2016. Structural ordering and dielectric properties of $Ba_3CaNb_2O_9$-based microwave ceramics. *Ceramics International* 42(16): 18087-18093.

Roulland, F. and Marinel, S. 2006. $Ba(Zn_{1/3}Nb_{2/3})O_3$ sintering temperature lowering for silver co-sintering applications, *Ceramics International* 32(4): 377-383.

Roulland, F., Terras, R., Allainmat, G., Pollet, M. and Marinel, S. 2004. Lowering of $Ba B'_{1/3}B''_{2/3}O_3$ complex perovskite sintering temperature by lithium salt additions. *Journal of the European Ceramic Society* 24(6): 1019-1023.

Roy, R. 1954. Multiple ion substitution in the perovskite lattice. *Journal of American Ceramic Society* 37: 581-588.

Sahin, E.I., Emek, M., Kartal, M., Pinar, S.K., Kargin, S. and Cantürk, S.B. 2020. Production and dielectric properties of Ta doped $Ba(Zn_{1/3}Nb_{2/3})O_3$ ceramics. *Ejons IX: International Conference on Mathematics, Engineering, Natural and Medical Sciences* : 107-113.

Sailaja, J.M., Babu, K.V., Murali, N. and Veeraiah, V. 2017. Effect of strontium on Nd doped $Ba_{1-x}Sr_xCe_{0.65}Zr_{0.25}Nd_{0.1}O_{3-\delta}$ proton conductor as an electrolyte for solid oxide fuel cells. *Journal of Advanced Research* 8(3): 169-181.

Scotta, R.I., Thomasa, M. and Hampsonb, C. 2003. Development of low cost, high performance $Ba(Zn_{1/3}Nb_{2/3})O_3$ based materials for microwave resonator applications, *Journal of the European Ceramic Society* 23: 2467–2471.

Sebastian, M.T. 2008. Introduction. In *Dielectric Materials for Wireless Communication*, ed. M.T. Sebastian, pp 1-10. Jordon Hill: Oxford.

Sebastian, M.T. 2008. Measurement of microwave dielectric properties and factors affecting them. In *Dielectric Materials for Wireless Communication*, ed. M.T. Sebastian, pp 11-47. Jordon Hill: Oxford.

Sebastian, M.T. 2008. $A(B'_{1/3}B''_{2/3})O_3$ complex perovskites. In *Dielectric Materials for Wireless Communication*, ed. M.T. Sebastian, pp 261-334. Jordon Hill: Oxford.

Sebastian, M.T. 2008. Low temperature cofired ceramics. In *Dielectric Materials for Wireless Communication*, ed. M.T. Sebastian, pp 445-512. Jordon Hill: Oxford.

Sebastian, M.T. and Surendran, K.P. 2006. Tailoring the microwave dielectric properties of $Ba(Mg_{1/3}Ta_{2/3})O_3$ ceramics. *Journal of the European Ceramic Society* 26(10-11): 1791-1799.

Sebastian, M.T., Jantunen, H. and Ubic, R. 2017. Perovskites. In *Microwave materials and applications*, ed. M.T. Sebastian, H. Jantunen, and R. Ubic, pp 81-148. New Jersey: John Wiley & Sons, Ltd.

Sebastian, M.T., Ubic, R. and Jantunen, H. 2015. Low-loss dielectric ceramic materials and their properties. *International Materials Reviews* 60(7): 392-412.

Senthil, V., Badapanda, T., Bose, A.C. and Panigrahi, S. 2016. Relaxation and conduction mechanism of Dy^{3+} substituted $SrBi_2Ta_2O_9$ ceramics. *Journal of Materials Science: Materials in Electronics* 27: 4760-4770.

Setter, N. and Waser, R. 2000. Electroceramic material. *Acta Materialia* 48(1): 151-178.

Shannon, R.D. 1993. Dielectric polarizabilities of ions in oxides and fluorides. *Journal of Applied Physics* 73: 348.

Shukleen, B.N., Kaur, D. and Pubby, K. 2015. Frequency and temperature dependence of dielectric and electric properties of $Ba_{2-x}Sm_{4+2x/3}Ti_8O_{24}$ with structural analysis. Materials Science-Poland 33(2): 268-277.

Sinclair, D.C. 1995. Characterization of electro-materials using ac impedance spectroscopy. *Journal of the Spanish Ceramic and Glass Society* 34(2): 55-66.

Sinclair, D.C., Morrison, F.D. and West, A.R. 2000. Applications of combined impedance and electric modulus spectroscopy to characterise electroceramics. *International Ceramics* 2: 33-38.

Sindam, B. and Raju, K.C.J. 2016. Microwave dielectric properties of $Ba(Zn_{1/3}Ta_{2/3})O_3$ for application in high power waveguide window. *The European Physical Journal B* 89(4): 92.

Sinha, R., Kundu, S., Basi, S. and Meikap, A.K. 2016. Effect of La doping on optical and electrical transport properties of nanocrystalline $YCrO_3$. *Solid State Sciences* 60: 75-84.

Sömiya, S. 1984. Electrical and electronic application. *In Advanced Technical Ceramics*, ed. S. Sömiya, pp 103-122. Academic Press Japan, Inc.

Srinivas, J., Dias, E.D. and Murthy, G.S. 1997. Crystal structure of $Ba(Mg_{1/3}Ta_{2/3})O_3$ calcinated at 1400°C. *Bulletin of Materials Science* 20(1): 23-25.

Srinivas, K., Sarah, P. and Suryanarayana, S.V. 2003. Impedance spectroscopy study of polycrystalline $Bi_6Fe_2Ti_3O_{18}$. *Bulletin of Materials Science* 26(2): 247-253.

Sun, T. L., Mao, M. M. and Chen, X. M. 2015. Structure and microwave dielectric properties of $Ba[(Mg_{1-x}Ni_x)_{1/3}Nb_{2/3}]O_3$ ceramics. *Materials Research Bulletin* 72: 291-298.

Sun, T. L., Zhao, Y. F. and Chen, X. M. 2015. Improvement of microwave dielectric properties for $Ba(Ni_{1/3}Nb_{2/3})O_3$ ceramics by Zr-Substitution. *Ceramics International* 41(4): 5872-5880.

Surendran, K.P., Sebastian, M.T., Mohanan, P. and Jacob, M.V. 2005. The effect of dopants on the microwave dielectric properties of $Ba(Mg_{0.33}Ta_{0.67})O_3$ ceramics. *Journal of Applied Physics* 98(9): 0941141.

Tamura, H., Konoike, T., Sakabe, Y. and Wakino, K. 1984. Improved high *Q* dielectric resonators with complex perovskite structure. *Journal of American Ceramic Society* 67: 59-61.

Tan, K.B., Khaw, C.C., Lee, C.K., Zainal, Z., Tan, Y.P. and Shaari, H. 2009. High temperature impedance spectroscopy study of non-stoichiometric bismuth zinc niobate pyrochlore. *Materials Science-Poland* 27(4/1): 947-959.

Thakur, S., Rai, R., Bdikin, I. and Valente, M.A. 2016. Impedance and modulus spectroscopy characterization of Tb modified $Bi_{0.8}A_{0.1}Pb_{0.1}Fe_{0.9}Ti_{0.1}O_3$ ceramics. *Materials Research* 19(1):1-8.

Thongbai, P., Jumpatam, J., Yamwong, T. and Maensiri, S. 2012. Effects of Ta^{5+} doping on microstructure evolution, dielectric properties and electrical response in $CaCu_3Ti_4O_{12}$ ceramics. *Journal of the European Ceramic Society* 32: 2423-2430.

Toderas, M., Filip, S. and Ardelean, I. 2006. Structural study of the Fe_2O_3-B_2O_3-BaO glass system by FTIR spectroscopy. *Journal of Optoelectronics and Advanced Materials* 8(3):1121-1123.

Varma, M.R., Reghunathan, R. and Sebastian, M.T. 2005. Effect of dopants on the microwave dielectric properties of $Ba(Zn_{1/3}Ta_{2/3})O_3$ ceramics. *Japanese Journal of Applied Physics* 44: 298-303.

Wang, Z., Huang, B., Wang, L., Fu, Z. and Zhang, Q. 2015. Low loss $(Ba_{1-x}Sr_x)(Co_{1/3}Nb_{2/3})O_3$ solid solution: phase evolution, microstructure and microwave dielectric properties. *Journal of Materials Science: Materials in Electronics* 26(6): 4273-4279.

West, A.R. 1999. Crystal defects, non-stoichiometry and solid solutions. In *Basic Solid State Chemistry*, ed. A.R. West, pp 211-260. New York: John Wiley & Sons, Ltd.

Widiarti, N., Suryana, L.A., Wijayati, N., Rahayu, E.F., Harjito, H., Wardhana, S.B., Prasetyoko, D. and Suprapto, S. 2017. Synthesis of $SrO.SiO_2$ Catalyst and Its Application in the Transesterification Reactions of Soybean Oil. *Bulletin of Chemical Reaction Engineering and Catalysis* 12 (2): 299-305.

Wiley, J. 2008. Infrared Spectroscopy. In *Characterization and Analysis of Polymers*, ed. J. Wiley, pp 89-108. Wiley-Interscience Publication.

Wu, H. and Davies, P.K. 2006. Influence of non-stoichiometry on the structure and properties of $Ba(Zn_{1/3}Nb_{2/3})O_3$ microwave dielectrics. I. Substitution of $Ba_3W_2O_9$. *Journal of American Ceramic Society* 89: 2239-2249.

Wu, H. and Davies, P.K. 2006. Influence of non-stoichiometry on the structure and properties of $Ba(Zn_{1/3}Nb_{2/3})O_3$ microwave dielectrics. IV. tuning τ_f and the part size dependence of Q x f. *Journal of American Ceramic Society* 89(7): 2271-2278.

Yadav, R.J. 2016. High temperature synthesis of barium zinc niobate with flux. *International Journal of Advanced Research and Development* 1(2): 61-64.

Yan, Y., Jiang, M., Song, J., Hao, C., Jin, Q., Han, S., Li, L., Zhang, J. and Yao., X. 2017. Dielectric and impedance studies on $(K_{0.5}Na_{0.5})NbO_3$-based ceramics. In *Advances in materials processing*, ed. Y. Han, pp 609-619. Springer Nature Singapore Pte, Ltd.

Yang, J.-I., Nahm, S., Choi, C.-H., Lee, H.-J. and Park, H.-M. 2002. Microstructure and microwave dielectric properties of $Ba(Zn_{1/3}Ta_{2/3})O_3$ with ZrO_2 addition. *Journal of American Ceramic Society* 85: 165-168.

Yang, J-I., Nahm, S., Choi, C-H., Lee, H-J., Kim, J-L. and Park, H-M. 2002. Effect of Ga_2O_3 on microstructure and microwave dielectric properties of $Ba(Zn_{1/3}Ta_{2/3})O_3$ ceramics. *Japanese Journal of Applied Physics* 41: 702-706.

Yoon, K.H., Kim, D.P. and Kim, E.S. 1994. Effect of $BaWO_4$ on the microwave dielectric properties of $Ba(Mg_{1/3}Ta_{2/3})O$ ceramics. *Journal of American Ceramic Society* 77(4): 1062-1066.

Zeng, H., Wu, Y., Zhang, J., Kong, C., Yue, M. and Zhou, S. 2013. Grain size dependent electrical resistivity of bulk nanocrystalline Gd metals. *Progress in Natural Science: Materials International* 23(1): 18-22.

Zhang, J., Yue, Z. and Li, L. 2017. Crystal structure, defect relaxation and microwave dielectric properties of $Ba[(Mg_{1/3}Nb_{2/3})_{1-x}Hf_x]O_3$ solid solutions. *Journal of American Ceramic Society* 1-8.

Zhang, S. 2016. Impedance spectroscopy on carbon-based materials for biological application. In *Biological and Biomedical Coating Handbook Applications*, ed. S. Zhang, pp 135-194. Advances in Materials Science and Engineering.